Available online at www.sciencedirect.com
SCIENCE DIRECT
Journal of Virological Methods 132 (2006) 146–153
Journal of Virological Methods
www.elsevier.com/locate/jviromet

Real-time RT-PCR and SYBR Green I melting curve analysis for the identification of *Plum pox virus* strains C, EA, and W: Effect of amplicon size, melt rate, and dye translocation

Aniko Varga, Delano James *

Sidney Laboratory, Canadian Food Inspection Agency, 8801 East Saanich Road, Sidney, BC, Canada V8L 1H3

Received 23 June 2005; received in revised form 23 September 2005; accepted 3 October 2005
Available online 15 November 2005

Abstract

Real-time RT-PCR and SYBR green I melt curve analysis of a 74 bp amplicon enabled identification of *Plum pox virus* strains C, EA, and W, with distinct T_m's associated with each strain. This test is a useful supplement to a real-time RT-PCR test described earlier that was used to distinguish PPV strains D and M. A longer fragment of 155 bp was not effective for strain identification. A simplified one-tube protocol, with dithiothreitol eliminated from the reaction, showed similar sensitivity when compared to a two-tube protocol. For melt curve analysis, a slower melt rate of 0.1 °C/s, compared to 0.4 °C/s, was effective for detecting weak amplicons, and improved resolution of the T_m of amplicons amplified simultaneously. SYBR green I was useful for duplex melt curve analysis. In repeated melt run treatments (total of 14) of a single sample containing co-amplified targets, complete translocation of SYBR green I was observed, going from a 74 bp fragment to a 114 bp fragment. The duration of the melt run may be a critical factor affecting SYBR green I binding and translocation, and its manipulation may facilitate improved resolution and simultaneous detection of multiple targets. This phenomenon may explain inconsistent SYBR green I fluorescence patterns associated with melt curve analysis of some amplicon complexes.

Keywords: Plum pox virus; Strain typing; Real-time RT-PCR; Melt curve analysis; Melt rate; SYBR green I translocation; SmartCycler®

1. Introduction

Real-time PCR with SYBR Green I melting curve analysis is a simple and reliable technique that has been effective for the detection and identification of various pathogens. These include *Leishmania* species (Nicolas et al., 2002), animal RNA viruses such as Norwalk-like viruses and viruses infecting penaeid shrimp (Beuret, 2004; Mouillesseaux et al., 2003), and plant RNA viruses such as *Plum pox virus* (PPV; Varga and James, 2005). This approach to real-time PCR can be adapted for quantitative analysis of the target(s) of interest (Papin et al., 2004). SYBR Green I dye binds non-specifically to double-stranded DNA by intercalation and/or minor groove binding (Lekanne Deprez et al., 2002; Mouillesseaux et al., 2003; Zipper et al., 2004). Specific identification may be achieved by melting curve analysis that can be used for identification at the species level (Nicolas et al., 2002), or even identification of strains of a virus pathogen (Varga and James, 2005).

SYBR green I based detection methods are reliable for detecting nucleic acid targets characterized by sequence variability. Papin et al. (2004) found that use of a probe based assay such as TaqMan resulted in failure to detect 47% of possible single nucleotide variants of West Nile virus, whereas a SYBR green I based assay was just as sensitive, and more importantly, it detected 100% of possible variants. Richards et al. (2004) indicated that in the case of Noroviruses, the use of degenerate primers facilitate broad spectrum detection but that probe-type approaches such as TaqMan require high complementarity for probe binding. This may result in failure to detect viruses that have high sequence variability in the probe-binding region. This uncertainty or false negative result is unacceptable in situations where; (a) the result might affect early initiation of treatment which could make the difference between life and death, and (b) where a false negative result might contribute to the release/introduction of plants infected with pathogens, such as aphid-vectored PPV (Avinent et al., 1994), that may

* Corresponding author. Tel.: +1 250 363 6650x235; fax: +1 250 363 6661.
E-mail address: jamesd@inspection.gc.ca (D. James).

0166-0934/$ – see front matter.
doi:10.1016/j.jviromet.2005.10.004

be spread to other hosts in the vicinity. Other advantages of SYBR green-based real-time PCR assays include; easy identification of spurious or non-specific amplification, the ability to detect uncharacterized variants, and reduced time for analysis (Papin et al., 2004; Richards et al., 2004; Varga and James, 2005).

PPV is considered the most serious disease affecting stone fruits, members of the *Prunus* spp. (Nemeth, 1986). There are six recognized strains of PPV including D, M, EA, C, Rec, and W (Wetzel et al., 1991b; Cambra et al., 1994; Nemchinov et al., 1998; Glasa et al., 2004; James and Varga, 2005). These strains vary in aphid transmission, geographic distribution, host range, and pathogenicity, so strain identification is essential for effective control of the virus and improved understanding of the epidemiology of the associated disease.

Varga and James (2005) recently described a real-time multiplex PCR assay using SYBR green I and melt curve analysis for identification of members of the two major strains of PPV, strains D and M. This approach is relatively simple, and more rapid than previously described PPV strain typing methods including RT-PCR with RFLP analysis (Wetzel et al., 1991a), and integrated RT-PCR/nested PCR (Szemes et al., 2001). Varga and James (2005) demonstrated reliable identification of isolates of strain D and M in both herbaceous and woody hosts. Strain specific forward primers amplifying fragments of different sizes were combined with universal PPV primers, and primers targeting the endogenous NADH dehydrogenase gene (Menzel et al., 2002), in a multiplex system. This facilitated simultaneous PPV detection, D or M strain identification, and detection of an endogenous control that reduces false negative results. The 74 bp universal fragment, amplified for isolates of all PPV strains tested (Varga and James, 2005), had melting temperature characteristics with the potential to facilitate identification of isolates of strains other than D and M. In this study, real-time RT-PCR with SYBR green I melting curve analysis of the 74 bp fragment was evaluated for supplementary use in the identification of PPV strains C, EA, and W. Fragment size was assessed for efficacy by comparisons of the 74 bp fragment with a 155 bp fragment. Also, factors such as melt rate and the phenomenon of dye translocation were assessed for their effects on reliable detection and strain identification of PPV.

2. Materials and methods

2.1. Virus source

PPV C (a sweet cherry isolate) and PPV EA (El Amar) were obtained as freeze dried tissue samples from A. Myrta, Italy. These isolates were maintained in the herbaceous host *Nicotiana benthamiana*. PPV 2630 (D-2630) is a Canadian type D isolate mechanically sap-transmitted from peach (*Prunus persica* var. Redhaven) to *N. benthamiana.* The virus isolate W3174 is a Canadian isolate of PPV detected in plum (*Prunus domestica*), and mechanically sap-transmitted to *N. benthamiana*. This isolate represents a new strain of PPV, strain W (James and Varga, 2005).

2.2. Test design

PPV strain typing in this study is based on SYBR green I melt curve analysis of a single amplicon using a system similar to that developed in the PPV multiplex assay described by Varga and James (2005). Two universal amplicons (74 bp and 155 bp) were compared for their effectiveness and use in identification of PPV strains C, EA, and W. The PPV P1 oligonucleotide primer (Wetzel et al., 1991a), PPV-U, and PPV-RR primer sequences (in 5′ to 3′ orientation) are; ACCGAGACCACTACACTCCC, TGAAGGCAGCAGCATTGAGA, and CTCTTCTTGTGTTCCGACGTTTC, respectively. Attempts at specific identification and strain typing were carried out as follows; if the original multiplex assay (Varga and James, 2005) gave a positive result for PPV, but negative for D or M strain, a second real-time RT-PCR assay was performed with further analysis of the 74 bp or 155 bp universal amplicon, along with the internal amplification control (181 bp amplicon for the Nad5 gene).

2.3. Isolation of total RNA and real-time RT-PCR conditions

Total RNA (from fresh and/or freeze-dried herbaceous and/or woody leaf tissue, as required) was extracted as described by James et al. (2003). Two RT-PCR systems were assessed: (a) a two-tube system as described by Varga and James (2005); and (b) a one-tube system for increased simplicity and reduction of cross-contamination. The one-tube RT-PCR reaction was carried out without DTT, in a 25 μl volume. This consisted of 2.5 μl of a 1/10 water dilution of tRNA (herbaceous or woody) and 22.5 μl of master mix (2.5 μl of Karsai Buffer (Karsai et al., 2002), 0.5 μl each of 5 μM primers PPV-U, PPV-RR or PPV-P1, Nad5R, Nad5F and 10mM dNTP, 1 μl of 50 mM $MgCl_2$, 0.2 μl of RNaseOUT™ (40 U/μl, Invitrogen), 0.1 μl each of SUPERSCRIPT™ III (200 U/μl, Invitrogen) and Platinum® Taq DNA Polymerase High Fidelity (5 U/μl, Invitrogen), and 1 μl of 1:5000 (in TE pH 7.5) SYBR green I (Sigma) in 16.1 μl water). Real-time PCR was performed using a SmartCycler® II Thermal Cycler (Cepheid, Sunnyvale, CA) with data interpretation using SmartCycler® Software Version 2.0d. The one-tube cycling parameters consisted of a 10 min incubation at 50 °C followed by 2-step PCR: 2 min incubation at 95 °C followed by threshold-dependent cycling for 15 s at 95 °C, and 60 s at 60 °C, where cycling advanced to melt stage once total fluorescence passed threshold (manual setting of 20) plus an extra nine cycles. Fluorescence readings were taken during the anneal/extension step (60 °C incubation). Following threshold-dependent cycling, melting was performed from 60 to 95 °C at either 0.1 or 0.4 °C/s melt rates with a smooth curve setting averaging 1 point. Melting peaks were visualized by plotting the absolute value of the 1st derivative against the temperature. The melting temperature (T_m) was defined as the peak of the curve, and if the highest point was a plateau, then the midpoint was identified as the T_m. For electrophoretic analysis, PCR products (10 μl) were separated on a 1.5% agarose (BioRad) gel in TBE buffer, at 80 V for 60 min, with ethidium bromide staining.

3. Results

3.1. One tube real-time multiplex RT-PCR assay versus two-tube assay; sensivitity comparison

The one-tube real-time multiplex RT-PCR assay, as adapted from the two-tube procedure, was more sensitive with a broader range of detection. Amplification was observed with serially water-diluted total RNA extracts from infected herbaceous hosts, at 10^{-6} dilution (data not shown). Dilution of cDNA was no longer required with the one tube RT-PCR thus limiting and reducing any chance for contamination and/or technical error. This indicates a more robust reaction. Also, the initial cDNA synthesis reaction time was reduced from 60 to 10 min, with an overall reduction in assay time. Dithiothreitol (DTT), commonly added to enzyme mixtures for stabilization and/or maintaining activity, is a potential real-time PCR inhibitor that may delay cycle threshold (C_t) values (Pierce et al., 2002). DTT was removed from the one-tube assay with no loss in sensitivity observed.

3.2. SYBR green I translocation between amplicons

An interesting observation regarding melt peak analysis was made during sensitivity comparisons between the two-tube real-time multiplex RT-PCR versus the one-tube strain typing assay. Full translocation of SYBR green I from one amplicon to another was observed over repeated melt runs, during a time-course of melt analysis (Fig. 1A–D). Initially most of the SYBR green I was associated with the 74 bp fragment compared to the 114 bp D-specific fragment (Fig. 1A). However, following a total of 14 repeated melt runs on the same samples, the SYBR green I became almost completely associated with the 114 bp fragment and the melt peak for the 74 bp is barely discernable. Fig. 1A–D indicate melt number 1, 3, 8 and 14, respectively, clearly showing the relocation of the SYBR green I dye and accompanying fluorescence levels. Electrophoresis showed bands for both the 74 bp and 114 bp products (gel not shown).

3.3. Strain-specific T_m as a function of strain, amplicon size, and melt rate

The melting temperatures (T_m) of the 74 bp amplicons were distinct for C, EA, and W strains at both 0.1 and 0.4 °C/s melt rates (Fig. 2). Strain C had the lowest T_m (mean 79.84 °C/80.94 °C) while strain EA was highest (av. 81.27 °C/82.40 °C) at both the 0.1 and 0.4 °C/s melt rates, respectively (Fig. 2). Increasing the melt rate from 0.1 to 0.4 °C/s shifted the T_m higher across all strains, an average of approximately 1.08 °C. The shift in T_m was not constant across strains. The relative T_m difference between strains C and EA going from a melt rate of 0.1 to 0.4 °C/s was 1.43 and 1.46 °C, respectively (Fig. 2). The relative T_m difference for W3174 compared to EA was 0.59 and 0.85 °C at 0.1 and 0.4 °C/s melt rate, respectively. The relative T_m difference between C and W3174 was median at 1.02 and 0.91 °C at 0.1 and 0.4 °C/s, respectively.

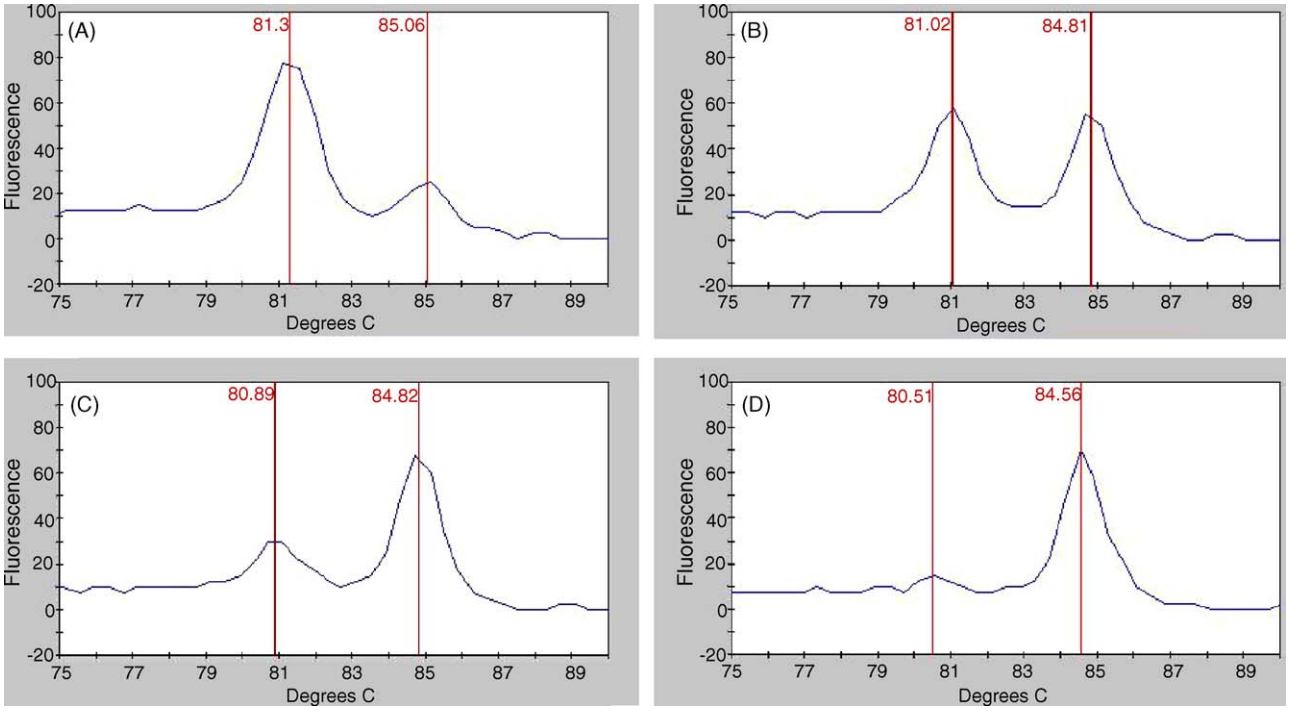

Fig. 1. Melt peak analysis of duplex targets over a series of melt runs showing translocation of SYBR green I over time. The reaction tube was subjected to a total of 14 consecutive melt runs, with A–D representing melt run number 1, 3, 8, and 14, respectively. After melt run number 1 (A), most SYBR green I is associated with the 74 bp fragment (T_m of 81.3 °C) while less is associated with the 114 bp fragment (T_m of 85.06 °C). After a total of 14 melt runs, most of the SYBR green is associated with the 114 bp amplicon (T_m of 84.56 °C) (D). Gel electrophoresis (1.5% agarose/TBE gel with Ethidium bromide staining) confirmed the presence of both amplicons.

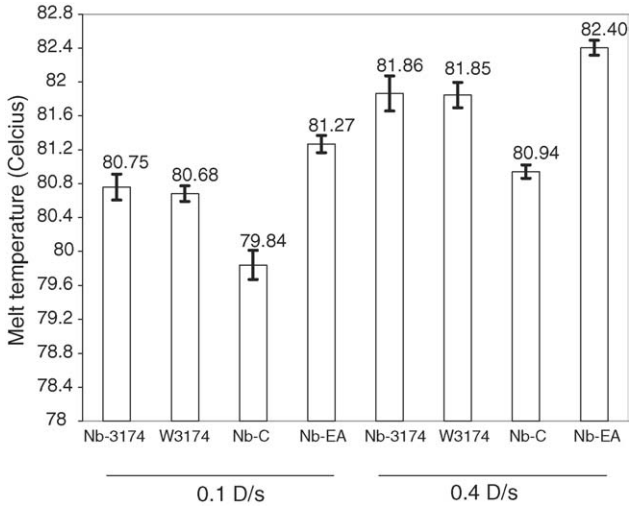

Fig. 2. Mean melting temperatures (°C ± S.D.) of the 74 bp fragment at 0.1 °C/s and 0.4 °C/s of strains W (Nb-3174 and W3174, herbaceous and woody hosts, respectively), C and EA (herbaceous hosts only). Nb indicates that the virus is present in the herbaceous host *Nicotiana benthamiana*. Means are representative of eight samples. Experiments were repeated at least two times.

The T_m's associated with the 155 bp amplicons were higher in general than that of the 74 bp fragment. There was some loss of resolution with overlap of the average T_m values of the three strains, at both ramp rates (Fig. 3). Overlapping T_m's occurred between strains W and EA, ranging from 84.94 to 85.95 °C. However it was possible to distinguish strain C, from EA and W. The strain C fragment has T_m's of 85.94 and 86.82 °C at melt rates of 0.1 and 0.4 °C/s, respectively, compared to 84.95–85.07 °C and 85.76–85.95 °C for EA and W at melt rates 0.1 and 0.4 °C/s, respectively (Fig. 3). The T_m was lowest for EA and W strains, and highest for strain C at both the 0.1 and 0.4 °C/s melt rates (Fig. 3). Increasing the melt rate from 0.1 to

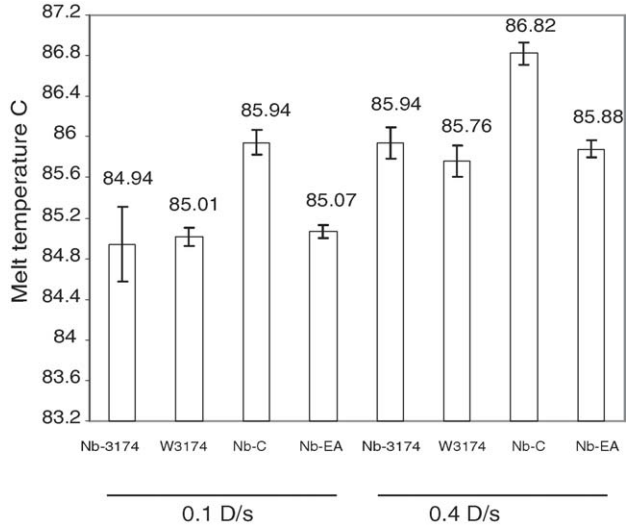

Fig. 3. Mean melting temperatures (°C ± S.D.) of the 155 bp fragment at 0.1 and 0.4 °C/s of strains W (Nb-3174 and W3174, herbaceous and woody hosts, respectively), C and EA (herbaceous hosts only). Nb indicates that the virus is present in the herbaceous host *Nicotiana benthamiana*. Means are representative of eight samples. Experiments were repeated at least two times.

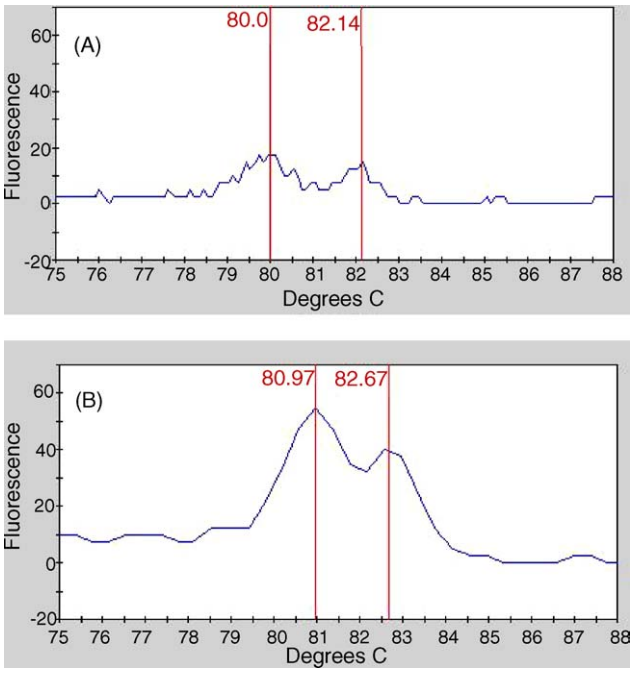

Fig. 4. Increase in melt peak resolution with increased melt rate. Following RT-PCR on C strain-infected herbaceous tissue (see methods), the reaction tube was subjected to two melt rates: 0.1 and 0.4 °C/s. At 0.1 °C/s melt rate (A), peaks for the 74 bp and 181 bp amplicons are small (T_m of 80.0 and 82.14 °C, respectively). At the 0.4 °C/s melt rate (B), peaks for the 74 bp and 181 bp amplicons are larger (T_m of 80.97 and 82.67 °C, respectively).

0.4 °C/s resulted in an upward shift of the T_m across all strains, on average 0.86 °C (Fig. 3). Again, the increase in T_m was not constant across all strains.

3.4. Influence of melt rate on the detection of weak amplicons

Following PCR amplification, samples were subjected to two melt runs, with melt rates of either 0.1 or 0.4 °C/s. Melt peaks were observed for both the 74 bp fragment (T_m of 80.0 °C) and 181 bp control fragment (T_m of 82.14 °C), at 0.1 °C/s (Fig. 4A). Larger more discernible melt peaks were associated with the 0.4 °C/s melt rate with T_m's of 80.97 and 82.67 °C for the 74 bp and 181 bp amplicons, respectively (Fig. 4B). Increasing the melt rate increased the size of the melt peaks due to a more rapid loss of fluorescence, facilitating more reliable detection of weaker amplicons (Fig. 4B). The typical T_m shift (lower to higher with increased melt rates) was observed.

3.5. Influence of melt rate on the discrimination of close T_m's

When two amplicons melt at similar temperatures, a slow melt rate (resulting in higher T_m resolution) resulted in improved discrimination of the melt peaks (Fig. 5). At a melt rate of 0.1 °C/s, melt peaks were observed for both the 74 bp amplicon (T_m 80.8 °C, strain W), and the 181 bp internal control fragment

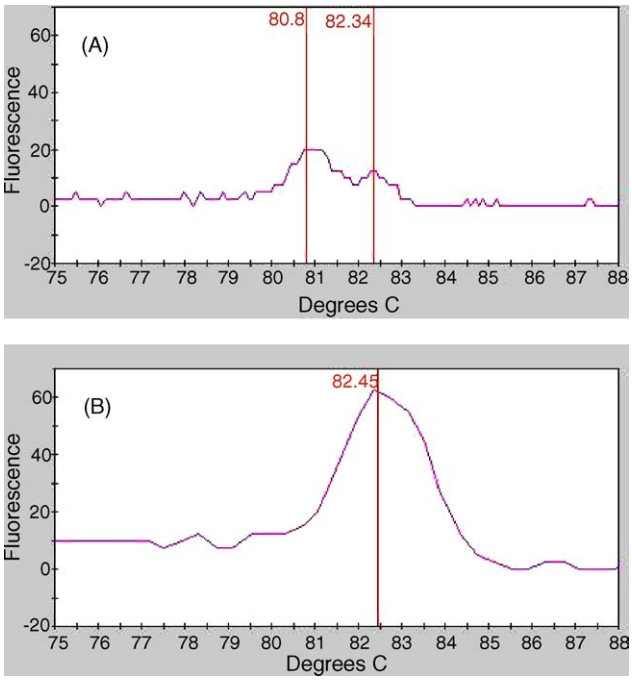

Fig. 5. Melt peak analysis showing a loss of resolution of weak amplicons with an increased melt rate, for strain W (fresh, woody tissue, a 1/40 water dilution of tRNA). Following RT-PCR, the reaction tube was subjected to two melt rates: 0.1 and 0.4 °C/s. At 0.1 °C/s (A), two melt peaks representing the 74 bp and 181 bp amplicons are observed (T_m's of 80.8 and 82.34 °C, respectively). At 0.4 °C/s (B), the melt peak temperature shifts higher and only one melt peak is discernible, representing the 181 bp amplicon with a T_m of 82.45 °C.

(T_m of 82.34 °C) (Fig. 5A). Though exhibiting higher fluorescence, only a single melt peak (T_m of 82.45 °C) was observed at a melt rate of 0.4 °C/s (Fig. 5B), indicating lower resolution of both amplicons. It appears that at the faster melt rate T_m's of all fragments are shifted higher, however, the increase in T_m does not appear equal between different fragments. This results in the T_m of one fragment approaching that of the second and becoming indistinguishable (Fig. 5B). This effect is reversible since if subjected to repeated melting at 0.1 °C/s melt rate, two melt peaks became visible (data not shown). The loss in peak resolution may be related also to both the increase in size, and temperature shift of melt peaks at higher melt rates (Figs. 4 and 5).

3.6. Influence of tissue type on T_m using the 74 bp and 155 bp fragments associated with strains W and D (D-2630)

The effects of host tissue type (leaves from herbaceous *N. benthamiana* or woody *Prunus* sp.) on T_m were determined for both the 74 bp and 155 bp fragments, at two melt rates. Two strains of PPV (W3174 and D-2630) were compared. Both are Canadian isolates that were available in fresh herbaceous and woody tissue. Strict quarantine regulations restrict the importation into Canada of *Prunus* infected with PPV strains C or EA, hence they were not evaluated. Herbaceous or woody host tissue type did not affect significantly the T_m associated with either the W3174 or D-2630 strain, for the 74 bp amplicon or the 155 bp amplicon, at either rate (Tables 1 and 2, respectively). An upward shift in T_m, with an increase in melt rate from 0.1 to 0.4 °C/s, was observed for the target in both hosts (Tables 1 and 2), indicating that the phenomenon is not host specific.

The effect on T_m of freeze drying herbaceous or woody tissue was examined, using tissue infected with strain W. In this case, there were no significant differences between the T_m observed for amplicons derived from RNA extracts from infected fresh herbaceous tissue, fresh woody tissue, or freeze-dried woody tissue (T_m °C ± S.D.) of 80.76 ± 0.15, 80.77 ± 0.16, and 80.68 ± 0.09, respectively). Freeze-dried herbaceous tissue was not tested.

Table 1
Mean melting temperatures (°C ± S.D.) of the 74 bp fragment at 0.1 and 0.4 °C/s of strains W3174 and D-2630 in herbaceous and woody hosts

0.1 D/s				0.4 D/s			
Nb-3174[a]	W3174[b]	Nb-2630[a]	D-2630[c]	Nb-3174[a]	W3174[b]	Nb-2630[a]	D-2630[c]
80.75 ± 0.15 (80.60–80.90)	80.68 ± 0.09 (80.59–80.77)	80.01 ± 0.19 (79.82–80.20)	79.89 ± 0.19 (79.70–80.08)	81.68 ± 0.21 (81.47–81.89)	81.85 ± 0.15 (81.70–82.00)	81.17 ± 0.11 (81.06–81.28)	80.97 ± 0.19 (80.78–81.16)

The range of melting temperatures is indicated in brackets.
[a] Herbaceous host Nicotiana benthamiana.
[b] Woody host Prunus domestica.
[c] Woody peach host, *Prunus persica* var. Redhaven. The mean was computed from a total of eight samples. Experiments were repeated at least twice.

Table 2
Mean melting temperatures (°C ± S.D.) of the 155 bp fragment at 0.1 °C/s and 0.4 °C/s of strains W3174 and D-2630 in herbaceous and woody hosts

0.1 D/s				0.4 D/s			
Nb-3174[a]	W3174[b]	Nb-2630[a]	D-2630[c]	Nb-3174[a]	W3174[b]	Nb-2630[a]	D-2630[c]
84.94 ± 0.36 (84.58–85.30)	85.01 ± 0.09 (84.92–85.10)	85.44 ± 0.13 (85.31–85.57)	85.46 ± 0.09 (85.37–85.55)	85.94 ± 0.16 (85.78–86.10)	85.76 ± 0.15 (85.61–85.91)	86.29 ± 0.11 (86.18–86.40)	86.29 ± 0.08 (86.21–86.37)

The range of melting temperatures is indicated in brackets.
[a] Herbaceous host Nicotiana benthamiana.
[b] Woody host Prunus domestica.
[c] Woody peach host, *Prunus persica* var. Redhaven. The mean was computed from a total of eight samples. Experiments were repeated at least twice.

4. Discussion

Real-time PCR is a powerful diagnostic tool capable of rapidly generating reliable and reproducible results with reduced risks of cross contamination (MacKay, 2004). In this study, single tube real-time RT-PCR with SYBR green I dye and melting curve analysis of a 74 bp amplicon were used for reliable identification of isolates of PPV strains C, EA, and W. When combined with the protocol described by Varga and James (2005) specific strain typing of members of all strains of PPV is possible, except strain PPV-Rec. PPV-Rec represents a group consisting of isolates that result from a recombination of PPV-D and PPV-M, with the PPV-M coat protein (CP) coding region at the 3′ terminus (Glasa et al., 2004). Based on sequence analysis, the procedure of Varga and James (2005), which targets the CP, will likely identify PPV-Rec as PPV-M. PPV-M is considered a severe (Kerlan and Dunez, 1979) and less desirable type of PPV. Any identification of PPV-M would trigger detailed analysis in the CP region and regions upstream such as the NIb and P3/6K1 region, which would facilitate identification of PPV-Rec (Glasa et al., 2002). Efforts to identify real-time RT-PCR strategies for simultaneous detection that include PPV-Rec are ongoing.

The real-time PCR approach described in this study utilizes the inexpensive dsDNA intercalating dye SYBR green I. There are two general approaches to amplicon detection, specific and non-specific fluorescent reporting chemistries. Both display similar levels of sensitivity (Wittwer et al., 1997; Bustin and Nolan, 2004a). The use of specific probe based assays such as TaqMan may result in false negative results, especially in RNA viruses (Papin et al., 2004; Richards et al., 2004), while non-specific assays using intercalating dyes such as SYBR Green I were found to be more reliable, flexible, simpler, and of lower costs (Papin et al., 2004; Richards et al., 2004; Varga and James, 2005). SYBR green I melt curve analysis is a useful detection tool (Hernandez et al., 2003; Richards et al., 2004; Beuret, 2004; Ririe et al., 1997) since it facilitates amplicon detection and differentiation, and has proven useful even in detecting single nucleotide polymorphism in duplex reactions (Papp et al., 2003).

Many plant pathogen molecular diagnostic tools fail introduction for routine use because of high costs, complexity, and lack of robustness (Martin et al., 2000). To increase simplicity, a one tube protocol adapted from a two tube procedure was developed, with no loss in sensitivity observed. The assay was reliable over a wide range of template (total RNA) concentrations, and there was a significant reduction in time (about 1 h), compared to the two-tube assay. Dithiothreitol was removed from the reaction mixture with no loss in sensitivity. DTT has been recognized to negatively interfere with RT-PCR using SYBR green I (Lekanne Deprez et al., 2002; Pierce et al., 2002). Other one-step RT-PCR protocols for RNA-virus detection have been optimized without DTT inclusion (Pastorino et al., 2005).

Complete translocation of SYBR green I dye from one amplicon to another was observed over a series of repeated melt runs on the same sample. This is an important phenomenon since it will be useful for improving the resolution of multiple targets in a single reaction, and possibly explains certain events observed in real-time PCR analysis. Fragments amplified in real-time PCR with melt curve analysis may be clearly visible on a gel, yet no associated melt peaks are observed. Two reports have shown discrepancies between melt peak data and gel electrophoresis (Giglio et al., 2003; Monis et al., 2005). Consequently concern was expressed about the reliability and usefulness of SYBR green I dye (Monis et al., 2005). It seems that too long a melt cycle may result in either translocation or preferential intercalation of SYBR green I with one fragment (represented by one melt peak), while more than one fragment is visible on a gel. A quicker melt cycle may remedy this anomaly. Monis et al. (2005) compared SYTO9 with SYBR green I for use in melt curve analyses. They used melt curve analyses settings of 1 °C steps with a hold of 10, 30, or 60 s at each step from 60 or 70 °C to 95 or 99 °C (depending on the loci), compared to the present study where 0.1 or 0.4 °C/sec melt rates (no hold) from 60 to 95 °C were used. In the study by Monis et al. (2005), a loss of one of the melt peaks was observed at either low SYBR green I concentrations or low template concentrations, however both amplicons (inferred from melt peak plots) were observed with SYTO9 across a broader range of dye concentrations and initial template DNA concentrations. In the present study, it seems that SYBR green I was not limiting but translocated from one amplicon to another after repeated melt runs (14 runs over 84 min). SYBR green I translocation (not preferential binding) is supported by the fact that the area under the curve of a melt peak is proportional to the amount of product (Wilhelm and Pingoud, 2003). As no new product is being generated during a melt run, the peak is growing only as a result of SYBR green I translocation. This suggests that the binding pattern of SYBR green I is time and temperature dependent. SYBR green I is effective in duplex (this study) or multiplex reactions (Varga and James, 2005) when melt curves are generated quickly, eliminating the translocation events.

Giglio et al. (2003) observed a similar translocation event between amplicons (*ctxAB* and *hyl*), with melt regimes of 20 or 40 cycles. The translocation of SYBR green I between the two loci may be an artifact of the melt settings. The melt protocol is stated as including a ramping rate of 1 °C/60 s, assumed to be a 60 s hold, which is similar to Monis et al. (2005). The data from the present study on PPV identification suggests that the duration of the melt run is a critical factor in SYBR green melt curve analysis. Translocation of SYBR green I during melt runs may be reduced by melting samples quickly, which may facilitate simultaneous detection of all amplicons. However, care must be taken if increasing melt rate (e.g., 0.1 to 0.4 °C/s or higher) as a loss in sensitivity detecting weak amplicons may occur.

Successful SYBR green I multiplex melt curve analyses appear to be associated with quicker melt runs than those used by Monis et al. (2005). Beuret (2004) used melt parameters consisting of 0s or 15s incubation times and temperature transition rates of 20 °C/s on ROCHE's LightCycler®; Hernandez et al. (2003), and Richards et al. (2004) used a melt transition rate of 0.2 °C/s on Cepheid's SmartCycler® and Applied Biosystems' ABI PRISM® 7700 (no hold time is given), respectively. Papp et al. (2003) used melt parameters consisting of 0.2 °C/min from 60 to 92 °C on the Applied Biosystems' ABI® 7000; while Varga and James (2005) used a melt transition rate of 0.1 °C/s on Cepheid's

SmartCycler® for multiplex analyses. Melt settings and optional parameters vary between thermocyclers (Bustin and Nolan, 2004b), thus confounding resolution and interpretation of SYBR green I melt curve analyses. SYTO9 may help in melting peak resolution where real-time machines require a hold setting at each melt temperature to equilibrate block-type machines using Peltier- or Joule-based technologies. SYBR green I and SYTO9 differ slightly in their spectral characteristics with optimal excitation/emission wavelengths of 497/520 nm and 485/498 nm (Molecular Probes/Invitrogen, Carlsbad), respectively. The spectral characteristics of the machine must be considered in deciding on the fluorescence dye suitable for optimal assay performance. For example, since the FAM channel on the SmartCycler® includes an excitation and emission maxima of 450–495 nm and 510–527 nm, respectively, optimal detection of SYTO9 (emission at 498 nm) would not be realised. Reliable and reproducible melt curve analysis may not depend solely on dye type (SYBR green I or SYTO9) but also on the different machine capabilities.

Melt rate has an impact on melt peak resolution. A higher melt rate decreases the number of readings over time, therefore, loss of fluorescence is larger than at a lower melt rate. In addition, a melt rate of 0.1 °C/s is more sensitive to changes in fluorescence than a 0.4 °C/s as four times more fluorescence readings are taken. Higher resolution of T_m's is accomplished at the slower rate of 0.1 °C/s, however, greater resolution of weak amplicons occurs at the higher rate, as the peaks are larger in size. A trade off exists where at a slower rate melt T_m accuracy is improved but at the expense of potentially missing the melt peak of weak amplicons. Conversely, at a higher rate the peaks are larger, but the T_m has a higher associated standard deviation. Further comparisons on different machines and associated software would determine if the resolution of weak amplicons is improved with increased melt rate, or if this is peculiar to the SmartCycler® interface. No literature is available examining the interaction of melt rate, hold settings, data acquisition and subsequent software analyses, and SYBR green I melt curve analysis in multiplex reactions.

Melt rate also affected the resolution of T_m's. At 0.1 °C/s melt rate, melt peaks were distinct giving an increased resolution of peaks, however, a loss of peak resolution occurred with a ramp rate of 0.4 °C/s when the T_m's of the two amplicons were close. This is related to the shift in T_m from low to high which is associated with a low to high shift in melt rate (Ririe et al., 1997), as well as the machine's optics and/or software interpretation of fluorescence data. The T_m shift is not even between amplicons consequently a melding of the peaks is observed. Further study is needed to elucidate this phenomenon with SYBR green I melt curve analyses, especially to determine if it is an artifact of instrumentation. The type of real-time instrument (ROCHE's LightCycler®, Applied Biosystems ABI PRISM® 7700, and Corbett's Rotor Gene 3000™) did have significant impacts on the C_t value when a Taqman probe/plasmid assay was performed (Donald et al., 2005). The resolution of melt curve analyses may also depend on real-time platform and/or software analysis.

Amplicon size was a critical factor in facilitating the discrimination of PPV strains. A smaller fragment improved specificity and allowed strain typing of C, EA, and W strains. This is in contrast to Mouillesseaux et al. (2003) where increased amplicon size improved specificity in the identification of two RNA-viruses infecting penaeid shrimp. One can predict the T_m of a DNA target using various programs (Panjkovich and Melo, 2005), however, actual T_m derived from SYBR green I melt curve analysis is dependent on many interacting factors such as; GC content, length, sequence composition (Ririe et al., 1997), SYBR green I concentration (Monis et al., 2005), template concentration (Ririe et al., 1997) as well as machine capabilities and melt run settings (Ririe et al., 1997; this study).

Tissue type had no significant impact on the T_m obtained from either herbaceous or woody tissue using strain W and D (2630) as models in this study. Nor was the T_m significantly affected by tissue preparation (fresh versus freeze drying) using strain W as a model. Minimal data exists on the effect of tissue type or tissue handling for plant virus differentiation (based on T_m) using SYBR green I melt curve analysis. Co-purification of tissue-specific endogenous contaminants (matrix components) from nucleic acid extraction was shown to impact C_t by differentially delaying C_t between four bovine housekeeping genes (Tichopad et al., 2004). They suggest DNA template is blocked by macromolecules such as polysaccharides or proteins that inhibit the reaction and cause a delay in the C_t. No significant differences were observed in T_m values between tissue types or preparations in this study.

In conclusion, a real-time RT-PCR procedure complementary to that described by Varga and James (2005) was developed for strain typing PPV strains C, EA, and W. The procedure is relatively simple and utilizes SYBR green with melting curve analysis of a single 74 bp fragment, with unique T_m's associated with each strain. This shorter 74 bp fragment was found to be more effective than a 155 bp fragment assessed in this study. Melt rate affects target detection in melt curve analysis, with a slower ramp rate (0.1 °C/s) producing more reliable detection of weak amplicons and better T_m resolution. In this study, tissue type or tissue treatment (fresh versus freeze drying) did not appear to affect T_m values. Perhaps the most important result of this study is the demonstration of SYBR green I translocation from one amplicon to another. This translocation phenomenon may be useful when improved resolution and simultaneous detection of multiple targets are required. To our knowledge, this is the first account documenting the translocation of SYBR green I fully from one amplicon to another. This melt curve analysis over a time-course (using repeated melt runs of approximately 6 min each) may mimic what is happening in other machines with melt runs that are typically much longer (20–80 min), as hold steps during melt rate may be longer to approach and maintain block uniformity in some cyclers.

Acknowledgements

We wish to express our gratitude to Arben Myrta for freeze dried samples of PPV C (a sweet cherry isolate) and PPV EA. Also, we would like to thank the CFIA St. Catherines PPV survey crew for providing samples of PPV W3174 and PPV D (2630).

References

Avinent, L., Hermoso de Mendoza, A., Llacer, G., 1994. Transmission of plum pox potyvirus in Spain. EPPO Bull. 24, 669–674.

Beuret, C., 2004. Simultaneous detection of enteric viruses by multiplex real-time RT-PCR. J. Virol. Methods 115, 1–8.

Bustin, S.A., Nolan, T., 2004a. Pitfalls of quantitative real-time reverse transcription polymerase chain reaction. J. Biomol. Tech. 15, 155–166.

Bustin, S.A., Nolan, T., 2004b. Instrumentation. A-Z of Quantitative PCR. In: Bustin, S.A. (Ed.). IUL Biotechnology Series, No. 5. International University Line, La Jolla, CA.

Cambra, M., Asenio, M., Gorris, M.T., Perez, E., Camarasa, E., Garcia, J.A., Moya, J.J., Lopez-Abella, D., Vela, C., Sanz, A., 1994. Detection of plum pox potyvirus using monoclonal antibodies to structural and non-structural proteins. EPPO Bull. 24, 569–577.

Donald, C.E., Qureshi, F., Burns, M.J., Holden, M.J., Blasic Jr., J.R., Woolford, A.J., 2005. An inter-platform repeatability study investigating real-time amplification of plasmid DNA. BMC Biotechnol. 5 (1), 15.

Giglio, S., Monis, P.T., Saint, C.P., 2003. Demonstration of preferential binding of SYBR Green I to specific DNA fragments in real-time multiplex PCR. Nucleic Acids Res. 31, e136.

Glasa, M., Marie-Jeanne, V., Moury, B., Kúdela, O., Quiot, J.-B., 2002. Molecular variability of the P3-6K$_1$ genomic region among geographically and biologically distinct isolates of *Plum pox virus*. Arch. Virol. 147, 563–575.

Glasa, M., Palkovics, L., Komínek, P., Labonne, G., Pittnerová, S., Kúdela, O., Candresse, T., Šubr, Z., 2004. Geographically and temporally distant natural recombinant isolates of *Plum pox virus* (PPV) are genetically similar and form a unique PPV subgroup. J. Gen. Virol. 85, 2671–2681.

Hernandez, M., Rodriguez-Lazaro, D., Esteve, T., Prat, S., Pla, M., 2003. Development of melting temperature-based SYBR Green I polymerase chain reaction methods for multiplex genetically modified organism detection. Anal. Biochem. 323, 164–170.

James, D., Varga, A., 2005. Nucleotide sequence analysis of Plum pox virus isolate W3174: evidence of a new strain. Virus Res. 110, 143–150.

James, D., Varga, A., Thompson, D., Hayes, S., 2003. Detection of a new and unusual isolate of *Plum pox potyvirus* in plum (*Prunus domestica*). Plant Dis. 87, 1119–1124.

Karsai, A., Muller, S., Platz, S., Hauser, M.T., 2002. Evaluation of a homemade SYBR green I reaction mixture for real-time PCR quantification of gene expression. Biotechniques 32, 790–792, 794–796.

Kerlan, C., Dunez, J., 1979. Différenciation biologique et sérologique de souches du virus de la sharka. Annales de Phytopathol. 11, 241–250.

Lekanne Deprez, R.H., Fijnvandraat, A.C., Ruijter, J.M., Moorman, A.F., 2002. Sensitivity and accuracy of quantitative real-time polymerase chain reaction using SYBR green I depends on cDNA synthesis conditions. Anal. Biochem. 307, 63–69.

Mackay, I.M., 2004. Real-time PCR in the microbiology laboratory. Clin. Microbiol. Infect. 10, 190–212.

Martin, R.R., James, D., Lévesque, C.A., 2000. Impacts of molecular diagnostic technologies on plant disease management. Annu. Rev. Phytopathol. 38, 207–239.

Menzel, W., Jelkmann, W., Maiss, E., 2002. Detection of four apple viruses by multiplex RT-PCR assays with coamplification of plant mRNA as internal control. J. Virol. Methods 99, 81–92.

Monis, P.T., Giglio, S., Saint, C.P., 2005. Comparison of SYTO9 and SYBR Green I for real-time polymerase chain reaction and investigation of the effect of dye concentration on amplification and DNA melting curve analysis. Anal. Biochem. 340, 24–34.

Mouillesseaux, K.P., Klimpel, K.R., Dhar, A.K., 2003. Improvement in the specificity and sensitivity of detection for the Taura syndrome virus and yellow head virus of penaeid shrimp by increasing the amplicon size in SYBR Green real-time RT-PCR. J. Virol. Methods 111, 121–127.

Nemchinov, L., Crescenzi, A., Hadidi, A., Piazzolla, P., Verderevskaya, T., 1998. Present status of the new cherry subgroup of plum pox virus (PPV-C). In: Hadidi, A., Khetarpal, R.K., Koganezawa, H. (Eds.), Plant Virus Disease Control. APS Press, St. Paul, Minnesota, pp. 629–638.

Nemeth, M., 1986. Plum pox (sharka). In: Virus, Mycoplasma and Rickettsia Diseases of Fruit Trees. Akademiai Kiado, Budapest, pp. 463–479.

Nicolas, L., Milon, G., Prina, E., 2002. Rapid differentiation of Old World *Leishmania* species by LightCycler polymerase chain reaction and melting curve analysis. J. Microbiol. Methods 51, 295–299.

Panjkovich, A., Melo, F., 2005. Comparison of different melting temperature calculation methods for short DNA sequences. Bioinformatics 21, 711–722.

Papin, J.F., Vahrson, W., Dittmer, D.P., 2004. SYBR Green-based real-time quantitative PCR assay for detection of West Nile virus circumvents false-negative results due to strain variability. J. Clin. Microbiol. 42, 1511–1518.

Papp, A.C., Pinsonneault, J.K., Cooke, G., Sadee, W., 2003. Single nucleotide polymorphism genotyping using allele-specific PCR and fluorescence melting curves. Biotechniques 34, 1068–1072.

Pastorino, B., Bessaud, M., Grandadam, M., Murri, S., Tolou, H.J., Peyrefitte, C.N., 2005. Development of a TaqMan RT-PCR assay without RNA extraction step for the detection and quantification of African Chikungunya viruses. J. Virol. Methods 124, 65–71.

Pierce, K.E., Rice, J.E., Sanchez, J.A., Wangh, L.J., 2002. QuantiLyse: reliable DNA amplification from single cells. Biotechniques 32, 1106–1111.

Ririe, K.M., Rasmussen, R.P., Wittwer, C.T., 1997. Product differentiation by analysis of DNA melting curves during the polymerase chain reaction. Anal. Biochem. 245, 154–160.

Richards, G.P., Watson, M.A., Kingsley, D.H., 2004. A SYBR green, real-time RT-PCR method to detect and quantitate Norwalk virus in stools. J. Virol. Methods 116, 63–70.

Szemes, M., Kálman, M., Myrta, A., Boscia, D., Németh, M., Kölber, M., Dorgai, L., 2001. Integrated RT-PCR/nested PCR diagnosis for differentiating between subgroups of plum pox virus. J. Virol. Methods 92, 165–175.

Tichopad, A., Didier, A., Pfaffl, M.W., 2004. Inhibition of real-time RT-PCR quantification due to tissue-specific contaminants. Mol. Cell. Probes 18, 45–50.

Varga, A., James, D., 2005. Detection and differentiation of Plum pox virus using real-time multiplex PCR with SYBR Green and melting curve analysis: a rapid method for strain typing. J. Virol. Methods 123, 213–220.

Wetzel, T., Candresse, T., Ravelonandro, M., Dunez, J., 1991a. A polymerase chain reaction assay adapted to plum pox potyvirus detection. J. Virol. Methods 33, 355–365.

Wetzel, T., Candresse, T., Ravelonandro, M., Delbos, R.P., Mazyad, H., Aboul-Ata, A.E., Dunez, J., 1991b. Nucleotide sequence of the 3′-terminal region of the RNA of the El Amar strain of plum pox potyvirus. J. Gen. Virol. 72, 1741–1746.

Wilhelm, J., Pingoud, A., 2003. Real-time polymerase chain reaction. Chem. Bio. Chem. 4, 1120–1128.

Wittwer, C.T., Herrmann, M.G., Moss, A.A., Rasmussen, R.P., 1997. Continuous fluorescence monitoring of rapid cycle DNA amplification. Biotechniques 22, 130–138.

Zipper, H., Brunner, H., Bernhagen, J., Vitzthum, F., 2004. Investigations on DNA intercalation and surface binding by SYBR Green I, its structure determination and methodological implications. Nucleic Acids Res. 32 (12), e103.